Microsolvation of the acetate anion [$CH_3CO_2^-(H_2O)_n$, $n = 1$–3]: A photoelectron spectroscopy and ab initio computational study

Xue-Bin Wang [a,b,*], Barbara Jagoda-Cwiklik [c], Chaoxian Chi [d], Xiao-Peng Xing [a,b], Mingfei Zhou [d], Pavel Jungwirth [e,*], Lai-Sheng Wang [a,b,*]

[a] Department of Physics, Washington State University, 2710 University Drive, Richland, WA 99354, USA
[b] Chemical and Materials Sciences Division, Pacific Northwest National Laboratory, MS K8-88, P.O. Box 999, Richland, WA 99352, USA
[c] The Fritz Haber Institute for Molecular Dynamics, The Hebrew University, Jerusalem 91904, Israel
[d] Department of Chemistry, Shanghai Key Laboratory of Molecular Catalysts and Innovative Materials, Advanced Materials Laboratory, Fudan University, Shanghai 200433, China
[e] Institute of Organic Chemistry and Biochemistry, Academy of Sciences of the Czech Republic, Center for Complex Molecular Systems and Biomolecules, Flemingovo nám. 2, 16610 Prague 6, Czech Republic

ARTICLE INFO

ABSTRACT

A combined photoelectron spectroscopy and ab initio theoretical study was carried out to study the microsolvation of the acetate anion. Photoelectron spectra of cold solvated clusters $CH_3CO_2^-(H_2O)_n$ ($n = 1$–3) at 12 K were obtained and compared with theoretical calculations. The first water is shown to bind to the $-CO_2^-$ group in a bidentate fashion, whereas both water–water and water-CO_2^- interactions are shown for $n = 2$ and 3. Significant rearrangement of the solvation structures is observed upon electron detachment, and water–CH_3 interactions are present for all the neutral clusters, $CH_3CO_2(H_2O)_n$ ($n = 1$–3).

© 2009 Elsevier B.V. All rights reserved.

1. Introduction

As a volatile organic acid, acetic acid has been found to be the most abundant species among organic compounds in the atmosphere [1]. Detailed knowledge of the dissolution of acetic acid and the solvation behavior of acetate may be valuable to understanding their chemistry in solution and the fate and transport of this environmental pollutant. Unlike simple diatomic salts or acids where charge–dipole and polarization interactions with polar solvents dictate the dissolution processes [2–7], acetate consists of a hydrophilic ($-CO_2^-$) and a hydrophobic ($-CH_3$) group, which may induce interesting solvation behaviors depending on the competition of hydrophilic and hydrophobic interactions. A recent molecular dynamic simulation shows acetate prefers the solution/vapor interface [8], where it is orientated such that the $-CO_2^-$ group is solvated below the interface while the methyl group is near or above the interface. Gas phase clusters with well-controlled solvent numbers provide ideal model systems to study the solute–solvent interactions at the molecular level [9–16]. For example, a nominally symmetrical binding motif between the $-CO_2^-$ group of acetate and one water molecule has been identified via IR action spectroscopy and theoretical modeling of $CH_3COO^-H_2O$, exhibiting importance of zero-point energy effects and vibrational adiabaticity [15,16]. We have carried out a series of investigations of micro-

solvation on a variety of complex anions [17–23] by combining photoelectron spectroscopy (PES) and ab initio calculations. In a number of studies [18–21], we have been able to extrapolate from cluster studies to behaviors at solution/vapor interfaces. Here we examine the microsolvation of the acetate anion, which, to the best of our knowledge, has not been studied previously.

2. Experimental methods

The experiment was performed using a low-temperature photoelectron spectroscopy (PES) apparatus, details of which have been published recently [24]. Briefly, the apparatus is equipped with an electrospray ionization source (ESI), a temperature-controlled ion trap, a time-of-flight (TOF) mass spectrometer, and a magnetic-bottle TOF photoelectron analyzer. Anions produced from the ESI source are guided by a RF-only quadruple ion guide and a quadruple mass filter into a 3D quadruple ion trap for ion accumulation and collisional cooling. The ion trap is attached to the cold head of a close-cycle helium refrigerator, and its temperature can be controlled between 12 and 350 K. In the current study, the coldest temperature of 12 K was used and the background cooling gas consisted of 0.1 mTorr helium mixed with 20% H_2. The cooled ions were pulsed into the extraction zone of the TOF mass spectrometer at a 10 Hz repetition rate. During PES experiment, the $CH_3CO_2^-(H_2O)_n$ ($n = 0$–3) ions were selected by a mass gate and decelerated before being intercepted by the 193 nm (6.424 eV) probing laser beam in the photodetachment zone. The emitted photoelectrons were collected at nearly 100% efficiency by the

* Corresponding authors. Address: Department of Physics, Washington State University, 2710 University Drive, Richland, WA 99354, USA.
E-mail addresses: xuebin.wang@pnl.gov (X.-B. Wang), pavel.jungwirth@uochb.cas.cz (P. Jungwirth), ls.wang@pnl.gov (L.-S. Wang).

magnetic bottle and analyzed in a 5.2-m long electron flight tube. Photoelectron TOF spectra were collected and then converted to kinetic energy spectra, calibrated by the known spectra of I^- and O^-. The electron binding energy spectra were obtained by subtracting the kinetic energy spectra from the detachment photon energy. We produced $CH_3CO_2^-(H_2O)_n$ ($n = 0$–3) clusters by electrospraying a 10^{-3} M sodium acetate solution in a H_2O/CH_3CN mixed solvent. The low-temperature ion trap was important to eliminate hot bands in PES spectra, resulting in sharper spectral threshold and more accurate electron binding energies [25,26]. The source conditions and the solution concentration were tuned to optimize each species before recording its PES spectrum. Hydrated $CH_3CO_2^-(H_2O)_n$ clusters with $n > 4$ were observed, but their mass intensities of the larger clusters were too weak to allow us to take their PES spectra.

3. Experimental results

Fig. 1 shows the 193 nm photoelectron spectra of $CH_3CO_2^-$ $(H_2O)_n$ ($n = 0$–3) taken at an ion trap temperature of 12 K. Higher resolution spectra of the acetate anion at 355 and 266 nm have been reported previously [27], showing two strong bands at 3.5 and 4.0 eV, and a weak broad tail in the threshold region at 266 nm. The latter was vibrationally-resolved at 355 nm under 70 K conditions, revealing a broad vibrational progression due to a large O–C–O angle change upon electron detachment. The 193 nm spectrum is similar to that at 266 nm with strong well-resolved bands, A and B, corresponding to the first and second excited of the neutral (CH_3CO_2). Vibrational features were discernible in the B band, which was resolved into a nice vibrational progression in the previous study at 266 nm [27]. Our previous 355 nm spectrum yielded an accurate adiabatic detachment energy (ADE) for acetate as 3.250 ± 0.010 eV for the ground state transition (X), which corresponds to the electron affinity of the acetyloxyl radical. However, the ground state transition (X) was not resolved at 193 nm, similar to that at 266 nm, due to its weak intensity and heavy overlap with the A band.

The PES spectra of the hydrated acetate clusters, $CH_3CO_2^-(H_2O)_n$ ($n = 1$–3), are similar to that of the bare acetate, except that the electron binding energies increase systematically due to solvent stabilization. The spectral features were also broadened as a function of solvation, probably due to solvent reorganization upon electron detachment. Since no vibrational structures were resolved in the 193 nm spectra, we could not obtain the ADEs for the hydrated acetate clusters. To help evaluate the spectral shift due to solvent stabilization, we estimated the apparent threshold detachment energy (TDE) by drawing a straight line along the rising edge of the A band and then adding the instrumental resolution to the intersection with the binding energy axis. The TDEs so obtained for $CH_3CO_2^-(H_2O)_n$ ($n = 0$–3) are given in Table 1, and they are marked as black vertical bars in Fig. 1. The TDE can be viewed as the upper limit of the corresponding ADE. For the bare acetate anion, its true ADE was measured at 355 nm previously as 3.250 eV, compared with the TDE of 3.38 eV. Nevertheless, the TDEs allow us to evaluate the systematic electron binding energy increase upon solvation. The incremental increase of electron binding energies, defined as TDE(n)–TDE($n - 1$), was 0.70, 0.47, and 0.45 eV for $n = 1$–3, respectively. The first water induces a much larger stabilization of 0.70 eV, whereas the effects of the second and third water are similar and significantly reduced.

4. Theoretical results and discussion

In order to obtain detailed molecular structures and understand how water interacts with $CH_3CO_2^-$ we performed ab initio calculations using the Gaussian03 package [28]. For each $CH_3CO_2^-(H_2O)_n$
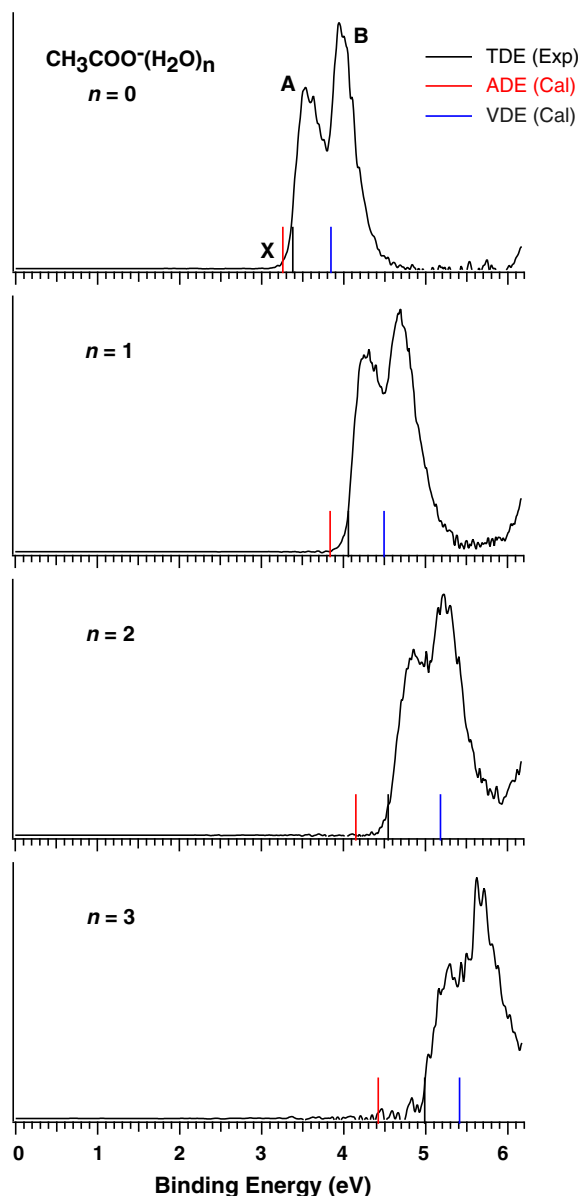

Fig. 1. Photoelectron spectra of $CH_3CO_2^-(H_2O)_n$ ($n = 0$–3) at 193 nm (6.424 eV) at 12 K. The experimental apparent threshold detachment energies (TDEs) and the calculated adiabatic (ADEs) and vertical (VDEs) detachment energies are shown as vertical bars in black, red and blue, respectively. (For interpretation of the references to colour in this figure legend, the reader is referred to the web version of this article.)

cluster we did geometry optimization without pre-imposed symmetry. We started from several different chemically reasonable structures in order to locate the global minimum. For the open-shell neutral species after electron detachment, full structural optimization was performed and for energetics projected values of unrestricted calculations were employed. Harmonic frequency analyses were performed for the optimized geometries to confirm that the obtained structures are minima on the potential energy surface. The lowest energy structures for both the anionic and neutral clusters are shown in Fig. 2.

4.1. Structures of $CH_3CO_2^-(H_2O)_n$ (n = 1–3) and the corresponding neutrals

The first water was found to form two H-bonds with $-CO_2^-$ in a bidentate fashion to optimize its interaction with the acetate

Table 1
Experimental threshold detachment energies (TDE's), calculated adiabatic (ADE's) and vertical (VDE's) detachment energies, and binding energies (E_W) of individual water molecules for $CH_3COO^-(H_2O)_n$ ($n = 0$–3) at MP2/aug-cc-pvdz level with projected MP2 energies considered (see text).

n	TDE (eV)[a]	ADE (eV)[b]	VDE (eV)[c]	E_W (kcal/mol)[d]
0	3.38(5)	3.24	3.86	–
1	4.08(5)	3.83	4.49	−19.6
2	4.55(5)	4.17	5.20	−17.0
3	5.00(5)	4.41	5.41	−17.1

[a] Obtained by drawing a straight line along the rising edge of the experimental A peak and then adding the instrumental resolution to the intersection with the binding energy axis. The numbers in parentheses represent the uncertainty in the last digit.
[b] Calculated as energy difference between the optimized anionic structure and that of neutral structure, corrected for the zero point energies evaluated at the respective minima of the anionic and neutral species.
[c] Calculated as the difference between the energy of the optimized anionic structure and that of the corresponding neutral at the anionic geometry.
[d] Calculated as the difference between the energy of the optimized anionic structure with n water molecules and the two fragments (i.e., a cluster with $n - 1$ water molecules and an isolated water molecule) at the same geometry; energies were corrected for the basis set superposition error.

(Fig. 2). Similar binding structure was reported previously via IR studies [15,16]. The association of the first water is very strong, with a binding energy of −19.6 kcal/mol (Table 1). After detaching the extra electron, this water experiences a large movement – rotating from the same plane with $-CO_2^-$ in the anionic form to being perpendicular with the $-CO_2$ plane, and forming only one H-bonding with one of the oxygen atom of the $-CO_2$ group, as well as weak interaction between the water oxygen and the CH_3 hydrogen (the corresponding distance is 2.50 Å). The binding energy of this water is much weaker (−4.2 kcal/mol) in the neutral species than that in

Fig. 2. Optimized structures of $CH_3CO_2^-(H_2O)_n$ ($n = 1$–3) and the corresponding neutral clusters.

the anionic state. In $CH_3CO_2^-(H_2O)_2$, the two water molecules behave in a similar way, both preferring to interact with the $-CO_2^-$ group. The two water molecules each form one O–H···O H-bond with a carboxylate O atom, as well as one inter-water H-bond with one water as the donor and the other as the acceptor (Fig. 2). The water–acetate binding energies are also very high for $n = 2$, i.e., −17.0 kcal/mol for each of the two waters. Again, large solvent relaxation is observed after removing the extra electron in the neutral cluster: one of the water molecules forms two H-bonds with the neutral $-CO_2$ end above its plane and also acts as a H-bond acceptor for the second water molecule, whose O atom simultaneously interacts with one of the H atoms in the methyl group with a distance of 2.29 Å (Fig. 2). Overall, the two water molecules interconnect together to bridge both ends of the neutral CH_3CO_2 radical. The C–H···O H-bond observed in neutral $CH_3CO_2(H_2O)_2$ is interesting. Such weak interactions are known be present in proteins [29] and have been observed to cause the formation of cyclic structures at low temperatures in long chain monocarboxylates, R-CO_2^- [25,30]. For the three water cluster, a similar solvation pattern emerges, where both solvent–solvent and solvent–CO_2^- interactions are observed. Interestingly, the three water molecules form a ring with each water acting both as a donor and acceptor, while each water also forms a H-bond with $-CO_2^-$. Such three-water ring structure has been observed to be an important solvation motif in hydrated sulfate clusters [31–34]. In the neutral, however, the water molecules again form a chain linking the $-CO_2$ and CH_3 group with a C–H···O H-bond (2.21 Å) (Fig. 2). The binding energy of the water molecules with acetate in $CH_3CO_2^-(H_2O)_3$ remains to be strong (−17.1 kcal/mol per H_2O), similar to the $n = 2$ cluster.

4.2. Calculated electron detachment energies and comparison with the experiment

For each cluster, we computed both the ADE and vertical electron detachment energy (VDE). The ADE was computed as the difference between energies of the optimized neutral and anion structures, while the VDE was calculated as the difference between the energy of the anion and that of the neutral at the anion geometry. MP2/aug-cc-pvdz (projected values of unrestricted calculations for the open shell neutral species), MP2/aug-cc-pvtz, and CCSD(T)/aug-cc-pvdz levels of theory were employed for bare acetate and the $n = 1$ cluster. The calculated ADEs are all within 0.17 eV at these different levels. Therefore, only MP2/aug-cc-pvdz calculations were performed for the large clusters. The calculated ADEs and VDEs are given in Table 1 and they are also shown as red (ADE) and blue (VDE) vertical bars in Fig. 1.

In our previous study [25], we computed the ADE of the bare acetate at various levels of theory. The calculated ADE of 3.24 eV at PMP2/aug-cc-pvdz level (Table 1) was in excellent agreement with the experimental ADE (3.250 ± 0.010 eV) [25]. Our current calculations predicted successive increases of the ADEs by 0.59 eV for the first water, 0.34 eV for the second, and 0.24 eV for the third water, consistent with the trend of the experimental observation. The calculations tend to overestimate the VDEs (Table 1 and blue vertical bars in Fig. 1) compared to the experimental values. This can be traced to possible problems due to the inaccurate description of the neutral radicals [35–37], where low lying excited states can mix in, particularly in non-minimal geometries. It should also be pointed out that the deviation between the calculated ADEs and experimental TDEs increases with the addition of water molecules, most likely due to increasing solvent relaxation upon detaching one electron from the anionic clusters. This observation was borne out from the large geometric changes from the anions to the neutrals (Fig. 2) and was also evidenced by the increase of the spectral width for larger clusters.
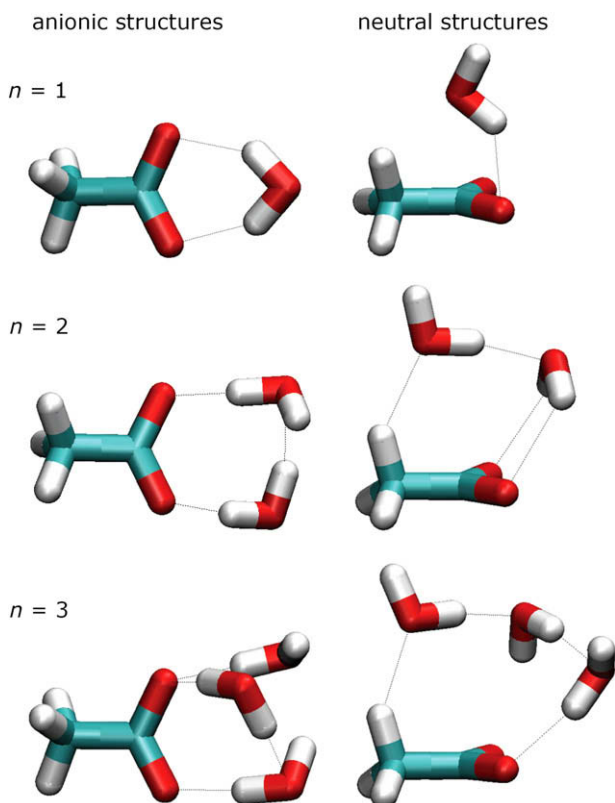
5. Concluding remarks

The solvated structures for $CH_3CO_2^-(H_2O)_n$ ($n = 1$–3) are clearly dominated by the hydrophilic interactions between H_2O and the $-CO_2^-$ group, similar to what we observed previously in the hydrated clusters of dicarboxylate dianions [20,21]. The water binding energies (17–19 kcal/mol) for the first three water molecules are quite high due to the negative charge in the $-CO_2^-$ group. The structures of the hydrated neutral CH_3CO_2 radical are interesting, clearly reflecting the competition between the hydrophobic and hydrophilic interactions. The removal of the negative charge on the carboxylate group significantly reduces the hydrophilic interactions with water, resulting in the rearrangement of the water molecules so that they can also interact with the CH_3 group. The acetyloxyl radical CH_3CO_2 is known to be unstable upon electron detachment of $CH_3CO_2^-$, dissociating into $CH_3 + CO_2$ [38]. In the hydrated acetyloxyl radical, the solvent molecules provide a link between the CH_3 and CO_2 groups and should stabilize the acetyloxyl radical against its dissociation compared to the bare one. The growth pattern revealed from the small solvated clusters can compare directly with the solvation behavior of acetate in aqueous solutions, revealing the preference of H_2O to the hydrophilic $-CO_2^-$. This solvation pattern is consistent with the behavior of acetate at the solution/vapor interface, where the hydrophobic CH_3 group is exposed [8].

Acknowledgments

References

[1] K. Kawamura, I.R. Kaplan, Environ. Sci. Technol. 17 (1983) 497;
    K. Kawamura, L.L. Ng, I.R. Kaplan, Environ. Sci. Technol. 19 (1985) 1082.
[2] S.M. Hurley, T.E. Dermota, D.P. Hydutsky, A.W. Castleman Jr., Science 298 (2002) 202.
[3] G. Gregoire, M. Mons, C. Dedonder-Lardeux, C. Jouvet, Eur. Phys. J. D 1 (1998) 5.
[4] D.E. Woon, T.H. Dunning, J. Am. Chem. Soc. 117 (1995) 1090.
[5] P. Jungwirth, D.J. Tobias, J. Phys. Chem. B 105 (2001) 10468.
[6] G.H. Peslherbe, B.M. Ladanyi, J.T. Hynes, J. Phys. Chem. A 104 (2000) 4533.
[7] A. Milet, C. Struniewicz, R. Moszynski, P.E.S. Wormer, J. Chem. Phys. 115 (2001) 349.
[8] B. Minofar, P. Jungwirth, M.R. Das, W. Kunz, S. Mahiuddin, J. Phys. Chem. C 111 (2007) 8242.
[9] G. Niedner-Schatteburg, V.E. Bondybey, Chem. Rev. 100 (2000) 4059.
[10] L. Lehr, M.T. Zanni, C. Frischkorn, R. Weinkauf, D.M. Neumark, Science 284 (1999) 635.
[11] O.M. Cabarcos, C.J. Weinheimer, J.M. Lisy, S.S. Xantheas, J. Chem. Phys. 110 (1999) 5.
[12] J.M. Papanikolas, J.R. Gord, N.E. Levinger, D. Ray, V. Vorsa, W.C. Lineberger, J. Phys. Chem. 95 (1991) 8028.
[13] A.T. Blades, P. Jayaweera, M.G. Ikonomou, P. Kebarle, J. Chem. Phys. 92 (1990) 5900.
[14] G. Markovich, S. Pollack, R. Giniger, O. Cheshnovsky, J. Chem. Phys. 101 (1994) 9344.
[15] W.H. Robertson, E.A. Price, J.M. Weber, J.-W. Shin, G.H. Weddle, M.A. Johnson, J. Phys. Chem. A 107 (2003) 6527.
[16] E.M. Myshakin, K.D. Jordan, E.L. Sibert III, M.A. Johnson, J. Chem. Phys. 119 (2003) 10138.
[17] X.B. Wang, X. Yang, L.S. Wang, Int. Rev. Phys. Chem. 21 (2002) 473.
[18] X.B. Wang, X. Yang, J.B. Nicholas, L.S. Wang, Science 294 (2001) 1322.
[19] X.B. Wang, X. Yang, J.B. Nicholas, L.S. Wang, J. Chem. Phys. 119 (2003) 3631.
[20] X. Yang, Y.J. Fu, X.B. Wang, P. Slavicek, M. Mucha, P. Jungwirth, L.S. Wang, J. Am. Chem. Soc. 126 (2004) 876.
[21] B. Minofar, M. Mucha, P. Jungwirth, X. Yang, Y.J. Fu, X.B. Wang, L.S. Wang, J. Am. Chem. Soc. 126 (2004) 11691.
[22] X.B. Wang, H.K. Woo, B. Jagoda-Cwiklik, P. Jungwirth, L.S. Wang, Phys. Chem. Chem. Phys. 8 (2006) 4294.
[23] X.B. Wang, X. Yang, L.S. Wang, J.B. Nicholas, J. Chem. Phys. 116 (2002) 561.
[24] X.B. Wang, L.S. Wang, Rev. Sci. Instrum. 79 (2008) 073108.
[25] X.B. Wang, H.K. Woo, B. Kiran, L.S. Wang, Angew. Chem. Int. Ed. 44 (2005) 4968.
[26] X.B. Wang, H.K. Woo, L.S. Wang, J. Chem. Phys. 123 (2005) 051106.
[27] X.B. Wang, K. Woo, L.S. Wang, B. Minofar, P. Jungwirth, J. Phys. Chem. A. 110 (2006) 5047.
[28] M.J. Frisch et al., GAUSSIAN 03 (Revision C.02), Gaussian, Inc., Wallingford, CT, 2004.
[29] R. Vargas, J. Garza, D.A. Dixon, B.P. Hay, J. Am. Chem. Soc. 122 (2000) 4750, and references therein.
[30] H.K. Woo, X.B. Wang, B. Kiran, L.S. Wang, J. Phys. Chem. A 109 (2005) 11395.
[31] X.B. Wang, J.B. Nicholas, L.S. Wang, J. Chem. Phys. 113 (2000) 10837.
[32] J. Zhou, G. Santambrogio, M. Brümmer, D.T. Moore, L. Wöste, G. Meijer, D.M. Neumark, K.R. Asmis, J. Chem. Phys. 125 (2006) 111102.
[33] B. Gao, Z.F. Liu, J. Chem. Phys. 123 (2005) 224302.
[34] X.B. Wang, A.P. Sergeeva, J. Yang, J.P. Xing, A.I. Boldyrev, L.S. Wang, Phys. Chem. A. 113 (2009) 5567.
[35] A. Rauk, D. Yu, D.A. Armstrong, J. Am. Chem. Soc. 116 (1994) 8222.
[36] D. Yu, A. Rauk, D.A. Armstrong, J. Chem. Soc. Perkin Trans. 2 (1994) 2207.
[37] R.D. Bach, P.Y. Ayala, H.B. Schlegel, J. Am. Chem. Soc. 118 (1996) 12758.
[38] Z. Lu, R.E. Continetti, J. Phys. Chem. A 108 (2004) 9962.